JACS
JOURNAL OF THE AMERICAN CHEMICAL SOCIETY
Communication
pubs.acs.org/JACS

An Alkaline-Stable, Metal Hydroxide Mimicking Metal–Organic Framework for Efficient Electrocatalytic Oxygen Evolution

Xue-Feng Lu,[‡] Pei-Qin Liao,[‡] Jia-Wei Wang, Jun-Xi Wu, Xun-Wei Chen, Chun-Ting He, Jie-Peng Zhang,* Gao-Ren Li,* and Xiao-Ming Chen

MOE Key Laboratory of Bioinorganic and Synthetic Chemistry, KLGHEI of Environment and Energy Chemistry, School of Chemistry and Chemical Engineering, Sun Yat-Sen University, Guangzhou 510275, China

Supporting Information

ABSTRACT: Postsynthetic ion exchange of $[Co_2(\mu\text{-}Cl)_2(btta)]$ (MAF-X27-Cl, H_2bbta =1*H*,5*H*-benzo(1,2-*d*:4,5-*d*′)bistriazole) possessing open metal sites on its pore surface yields a material $[Co_2(\mu\text{-}OH)_2(bbta)]$ (MAF-X27-OH) functionalized by both open metal sites and hydroxide ligands, giving drastically improved electrocatalytic activities for the oxygen evolution reaction (an overpotential of 292 mV at 10.0 mA cm^{-2} in 1.0 M KOH solution). Isotope tracing experiments further confirm that the hydroxide ligands are involved in the OER process to provide a low-energy intraframework coupling pathway.

The electrochemical oxygen evolution reaction (OER) is the core process for a number of renewable energy systems such as metal–air batteries and water splitting.[1−3] As a four-electron process, OER always suffers from slow kinetics and needs high-performance catalysts to reduce the electrochemical overpotential.[4] Precious metal oxides, IrO_2 and RuO_2, are so far the most efficient OER catalysts, but their high cost and scarcity, as well as low durability are impractical for large-scale applications.[5,6] Other OER catalysts (mostly metal oxides/hydroxides)[7] generally show unsatisfactory catalytic activities with overpotentials of ca. 350−500 mV at 10 mA cm^{-2} (expected for a 10% efficient solar-to-fuels conversion device)[5,6,8−10] at pH = 14.

To improve the electrocatalytic performance, general strategies consider the catalyst particle size/morphology (surface structure and area), catalyst/electrode contact (electrical conductivity), composite effect, etc.[1,11,12] Obviously, the chemical structure of the electrocatalyst especially on the solid/liquid interface is the most fundamental issue.[13] However, the surface structures of conventional catalysts are usually different from those deduced from their crystal structures and difficult to determine directly.[14] For example, while the metal atom/ion plays a critical role for OER because it coordinates and discharges the H_2O/OH^- species, the particle surfaces exhibit predominantly as metal oxides,[7] or more accurately hydroxides in the aqueous, strongly oxidizing environment.[15] It has been proposed by computational simulation that the surface hydroxide ligands can have a lower energy barrier than an external (solution) H_2O/OH^- to couple with the discharged species,[16] but the advantage of such an intraframework coupling pathway has not been experimentally verified or rationally utilized because of the uncertain and uncontrollable catalyst surface structures.

Metal–organic frameworks (MOFs) are very attractive as catalysts for their highly ordered structures, large porosities, and diversified pore surfaces.[17−20] Especially, their surfaces are mostly contributed from the highly ordered internal pores as observed in the crystal structures, which are not only beneficial for mechanism study but also can be easily functionalized by open metal sites (OMSs) with Lewis acidity and/or redox property.[21−24] Some MOFs have been used as precursors to fabricate metal oxide/porous carbon nanocomposites as OER catalysts.[25−28] However, it seems that MOFs themselves are unsuitable as OER catalysts,[29−32] considering their poor stabilities (in water, especially basic/acidic conditions) and low electrical conductivities. Here, we report a strategy to integrate the advantages of metal oxides/hydroxides and MOFs. An open framework consisting of cobalt hydroxide chains is synthesized by metathesis of its cobalt chloride analogue, giving not only drastically improved OER activities but also a direct proof of the advantage of hydroxide ligand via the intraframework coupling pathway.

We selected a metal azolate framework $[Co_2(\mu\text{-}Cl)_2(bbta)]$ (MAF-X27-Cl in the guest-free form, H_2bbta =1*H*,5*H*-benzo-(1,2-d:4,5-d′)bistriazole) as an OER candidate, for the high stabilities of this kind of MOFs and its high-concentration (5.88 mmol g^{-1}, 6.69 mmol cm^{-3}), oxidizable OMSs (from Co(II)-Null to Co(II)-OH_2 or Co(III)-OH) (Figure 1).[33] Chemical stability tests showed that MAF-X27-Cl could retain its original crystallinity in acidic (0.001 M HCl) or strong alkaline (1.0 M KOH) solution for at least 1 week (Figure S1). Such a high chemical stability has been rarely reported for MOFs.[34−36]

Linear sweep voltammetry (LSV) was performed at pH = 14 for MAF-X27-Cl (microcrystalline powder coated on glassy-carbon electrode (GCE) with Nafion binder). By repeating the LSV, the OER performance increased gradually and finally (after 24 h) reached an overpotential of 387 mV at 10 mA cm^{-2}, being 121 mV lower than for the initial sample (Figure S2). X-ray photoelectron spectroscopy (XPS) analyses of MAF-X27-Cl after LSV tests showed that the Cl content disappeared, while the O content increased (Figure S3). Also, the color of the catalyst changed from pink to light pink, indicating that the Cl^- ligand of MAF-X27-Cl might be replaced by OH^-, giving a new catalyst $[Co_2(\mu\text{-}OH)_2(bbta)]$ (MAF-X27-OH in the guest-free form). Further experiments showed that the modification could be furnished by immersing MAF-X27-Cl in a solution of 1.0 M

Received: March 25, 2016
Published: June 29, 2016

DOI: 10.1021/jacs.6b03125
J. Am. Chem. Soc. 2016, 138, 8336–8339

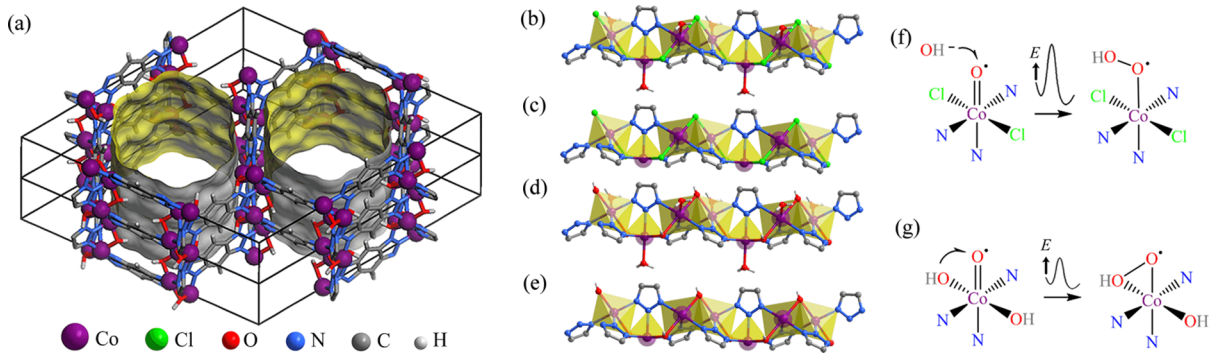

Figure 1. (a) Three-dimensional coordination network and pore surface structures of MAF-X27-OH. (b–e) Local coordination environments of (b) water-appended MAF-X27-Cl, (c) guest-free MAF-X27-Cl, (d) water-appended MAF-X27-OH, and (e) guest-free MAF-X27-OH. (f) Solid–liquid coupling pathway for MAF-X27-Cl. (g) Intraframework coupling pathway for MAF-X27-OH.

KOH for 24 h at room temperature without application of electric field (Figure S4 and Table S1). Raman spectroscopy of MAF-X27-OH (Figure 2) showed stretching vibration of Co–O

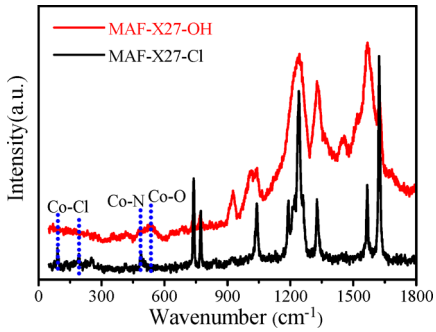

Figure 2. Raman spectra of MAF-X27-Cl and MAF-X27-OH.

at 536 cm^{-1} instead of Co–Cl at 92 and 195 cm^{-1}.[37,38] Scanning electron microscopy (SEM) and transmission electron microscope (TEM) images showed that MAF-X27-Cl and MAF-X27-OH had the same morphologies (Figure S5), indicating that the structural transformation occurs topochemically.

Thermogravimetry (Figure S6) and powder X-ray diffraction (PXRD, Figure S1) showed that MAF-X27-OH could release all guest solvent molecules below ca. 200 °C with retention of high crystallinity. Rietveld refinements of the PXRD patterns of their guest-free samples, without any restriction on the supramolecular structures, confirmed that MAF-X27-OH was isostructural with MAF-X27-Cl, and the μ-Cl^- (Co–Cl (2.406(6) Å) ligands were completely replaced by the μ-OH^- (Co–O 1.939(5) Å) ones (Figure S7). After ion exchange, the cell volume was reduced ca. 2%, which can be explained by the shorter Co–O coordination bonds (Table S2). Each Co(II) ion in MAF-X27-OH/MAF-X27-Cl is coordinated by three nitrogen atoms and two OH^-/Cl^- anions in a square-pyramidal geometry, with the pyramid base or the OMS facing toward the channel center (Figure 1). It could be expected that the Co(II) OMS within MAF-X27-OH can coordinate with a terminal H_2O/OH^- ligand and can be further oxidized to Co(III)-OH species, being similar for MAF-X27-Cl.[33] The terminal monodentate H_2O/OH^- or oxo ligand furnishes the octahedral coordination geometry of the Co ion and is very close (<3 Å) to two μ-OH^- ligands locating at its *cis*-positions (Table S2), being suitable for the intraframework coupling. N_2 sorption isotherms gave apparent Langmuir surface areas of 1407 and 1514 $m^2\ g^{-1}$ and pore volumes of 0.50 and 0.55 $cm^3\ g^{-1}$ (crystallographic values 0.51 and 0.57 $cm^3\ g^{-1}$) for MAF-X27-Cl and MAF-X27-OH, respectively, demonstrating good sample crystallinity and purity (Figure S8 and Table S2). Notably, the surface areas of MAF-X27-Cl and MAF-X27-OH are much higher than for inorganic OER catalysts (<500 $m^2\ g^{-1}$).[1,39–41]

The effectiveness of the μ-OH^- ligand was unambiguously demonstrated by comparing the OER activities of MAF-X27-Cl and MAF-X27-OH at pH = 7. The colors of the two catalysts did not change after the OER tests, indicating retention of their structures. MAF-X27-Cl showed very poor OER activity, with only 0.028 mA cm^{-2} at the overpotential of 570 mV (Figure 3).

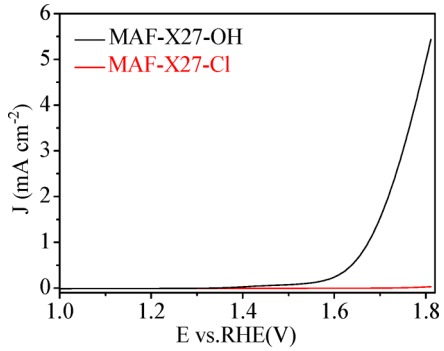

Figure 3. LSV curves of MAF-X27-Cl and MAF-X27-OH at pH = 7.

In contrast, MAF-X27-OH afforded a current density of 2.0 mA cm^{-2} at an overpotential of 489 mV (Figures 3 and S9), which is much better than all reported catalysts except $Co(PO_3)_2$ (410 mV) and $Co_3(PO_4)_2$ (460 mV) (Table S3). Further, the apparent electrochemical surface area of MAF-X27-OH was measured to be three times that of MAF-X27-Cl (Figure S10), highlighting the high activity of the modified material again. The electrical conductivities MAF-X27-OH and MAF-X27-Cl were measured to be 2.2×10^{-9} S cm^{-1} and 2.2×10^{-7} S cm^{-1}, respectively (Figure S11), being consistent with the relatively compact and loose electron clouds of OH^- and Cl^- anions[42] and indicates that the μ-OH^- ligand increases the electrocatalytic activity mainly by changing the chemical reaction pathway instead of the bulk electrical conductivity.[1,39] The OER mechanism of MAF-X27-OH was further studied by isotope tracing experiments. The IR stretching vibration of OD^- of MAF-X27-OD at 2672 cm^{-1} almost disappeared after an OER testing time of 15 min, accompanied with the appearance of the stretching vibration of OH^- at 3617 cm^{-1} (Figure S12).[43,44] In

DOI: 10.1021/jacs.6b03125
J. Am. Chem. Soc. 2016, 138, 8336–8339

contrast, the stretching vibration of OD^- was almost unchanged for 60 min without application of an electric field. These observations demonstrated the direct participation of the μ-OH^- ligand or the intraframework coupling pathway in the OER process. Considering that the OER performance of MAF-X27-OH is much higher than that of MAF-X27-Cl and the two isostructural materials have the same Co(II) OMSs for binding and oxidizing H_2O/OH^- species, this work provided direct evidence for the occurrence and advantage of the intraframework coupling mechanism.[45,46] XPS showed that the intensity of the Co 2p shake up peaks for MAF-X27-OH became weaker after the OER test, being consistent with the expected Co(II) to Co(III) oxidation (Figure S13). We also determined the concentration of Co^{2+} in the electrolyte after OER stability tests, which is below the detection limit of inductively coupled plasma atomic emission spectrometry (4 ng/mL), further confirming the high stability of MOF-X27-OH.

We further compared the OER activity of MAF-X27-OH with its inorganic analogues $Co(OH)_2$ and Co_3O_4 at pH = 14. Remarkably, microcrystals of MAF-X27-OH coated on GCE by Nafion (387 mV at 10 mA cm^{-2}) showed much better catalytic activity than nanocrystals of $Co(OH)_2$ (421 mV) and Co_3O_4 (445 mV) directly grown on carbon cloth substrates (Figures 4, S14, and S15 and Table S4).[47,48] It should be noted that, electrocatalysts grown directly on current collectors and/or composited with cocatalysts behave much better than their bulks (coated on GCE with Nafion binder) due to increases of electrical conductivity, reactant/product transportation, and other synergistic effects. For example, about 100 mV reduction of the overpotential have been observed for Co_3O_4/C-NA by changing the electrode preparation method from coating on GCE to directly grown on Cu foil and IrO_2 by forming a IrO_2/C composite (Table S4).[1,49−51] To more accurately evaluate the OER activity of MAF-X27-OH, we fabricated electrodes by growing the MOF crystals directly on Cu foil, hereafter denoted as MAF-X27-OH(Cu), by placing the substrate in the reaction system for synthesizing MAF-X27-Cl, followed by ion exchange treatment. Three electrodes with different morphologies and mass loadings were prepared (Figures S16−18), giving much improved OER performances with overpotentials as low as 292 mV at 10 mA cm^{-2} (Figure 4) and turnover frequency up to 0.019/0.25 s^{-1} at overpotential of 300/400 mV, being the best values among known catalysts (Table S4). Noted that the Faraday efficiency of MAF-X27-OH(Cu) for OER was also measured to be virtually 100% (Figures S19 and S20), confirming that the observed electrochemical data originates from water oxidation rather than other side reactions.

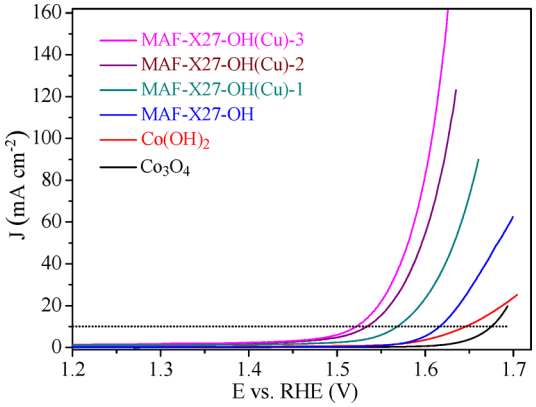

Figure 4. LSV curves of MAF-X27-OH, MAF-X27-OH(Cu) (samples 1−3), $Co(OH)_2$, and Co_3O_4 at pH = 14.

MAF-X27-OH also exhibits excellent durability in OER processes. The chronopotentiometric response of MAF-X27-OH showed a slight potential increase of 0.9% and 2.8% at 5 and 10 mA cm^{-2}, respectively, after 24 h due to the pelling of samples during the oxygen evolution, being superior to that of IrO_2/C (~45% increase at 10 mA cm^{-2} after 20 h)[1,52] under similar conditions (Figure S21). Furthermore, cyclic voltammetry curves, LSV curves, PXRD patterns, and SEM images of MAF-X27-OH showed negligible changes after OER tests for 24 h (Figure S22).

In summary, we discovered a MOF material that can work as good as high-performance inorganic OER catalysts in terms of both activity and stability/durability. By virtue of the tailorable/modifiable structure of the MOF, we were able to unambiguously compare the OER activities of two analogous materials bearing a simple metal surface and a metal hydroxide surface and confirm that the surface hydroxide ligand can greatly accelerate the reaction, which is not possible for inorganic metal and metal oxide/hydroxides because metal surfaces are always oxidized under OER environment. To obtain better electrochemical performances, further optimization of the crystal growth and/or composite/electrode structures can be subjected for the titled MOF material. These results and understandings may open up new possibilities for OER catalysts and related materials.

■ ASSOCIATED CONTENT

Supporting Information

The Supporting Information is available free of charge on the ACS Publications website at DOI: 10.1021/jacs.6b03125.

Experimental details and additional figures/tables (PDF)
X-ray crystallographic files (CIF)
X-ray crystallographic files (CIF)

■ AUTHOR INFORMATION

Corresponding Authors

*zhangjp7@mail.sysu.edu.cn
*ligaoren@mail.sysu.edu.cn

Author Contributions

‡These authors contributed equally to this work.

Notes

The authors declare no competing financial interest.

■ ACKNOWLEDGMENTS

This work was supported by the "973 Project" (2014CB845602 and 2015CB932304) and NSFC (21225105, 21290173, 51173212, and 21473260).

■ REFERENCES

(1) Ma, T. Y.; Dai, S.; Jaroniec, M.; Qiao, S. Z. *J. Am. Chem. Soc.* **2014**, *136*, 13925.
(2) Zhang, M.; de Respinis, M.; Frei, H. *Nat. Chem.* **2014**, *6*, 362.
(3) Kim, T. W.; Choi, K. S. *Science* **2014**, *343*, 990.
(4) Furlong, D.; Yates, D.; Healy, T.; Trasatti, S. *Electrodes of Conductive Metallic Oxides, Part B*; Elsevier, Amsterdam, 1981; p 367.
(5) McCrory, C. C.; Jung, S.; Ferrer, I. M.; Chatman, S. M.; Peters, J. C.; Jaramillo, T. F. *J. Am. Chem. Soc.* **2015**, *137*, 4347.
(6) McCrory, C. C.; Jung, S.; Peters, J. C.; Jaramillo, T. F. *J. Am. Chem. Soc.* **2013**, *135*, 16977.
(7) Minguzzi, A.; Fan, F.-R. F.; Vertova, A.; Rondinini, S.; Bard, A. J. *Chem. Sci.* **2012**, *3*, 217.

DOI: 10.1021/jacs.6b03125
J. Am. Chem. Soc. 2016, 138, 8336−8339

(8) Duan, J.; Chen, S.; Jaroniec, M.; Qiao, S. Z. *ACS Catal.* **2015**, *5*, 5207.
(9) Ma, T. Y.; Ran, J.; Dai, S.; Jaroniec, M.; Qiao, S. Z. *Angew. Chem., Int. Ed.* **2015**, *54*, 4646.
(10) Ma, T. Y.; Cao, J. L.; Jaroniec, M.; Qiao, S. Z. *Angew. Chem., Int. Ed.* **2016**, *55*, 1138.
(11) Xia, B. Y.; Yan, Y.; Li, N.; Wu, H. B.; Lou, X. W.; Wang, X. *Nat. Energy* **2016**, *1*, 15006.
(12) Lin, S.; Diercks, C. S.; Zhang, Y.-B.; Kornienko, N.; Nichols, E. M.; Zhao, Y.; Paris, A. R.; Kim, D.; Yang, P.; Yaghi, O. M.; Chang, C. J. *Science* **2015**, *349*, 1208.
(13) Plaisance, C. P.; van Santen, R. A. *J. Am. Chem. Soc.* **2015**, *137*, 14660.
(14) Wu, Y.; Chen, M.; Han, Y.; Luo, H.; Su, X.; Zhang, M.-T.; Lin, X.; Sun, J.; Wang, L.; Deng, L.; Zhang, W.; Cao, R. *Angew. Chem.* **2015**, *127*, 4952.
(15) Bockris, J. O.; Otagawa, T. *J. Phys. Chem.* **1983**, *87*, 2960.
(16) Mattioli, G.; Giannozzi, P.; Amore Bonapasta, A.; Guidoni, L. *J. Am. Chem. Soc.* **2013**, *135*, 15353.
(17) Lee, J.; Farha, O. K.; Roberts, J.; Scheidt, K. A.; Nguyen, S. T.; Hupp, J. T. *Chem. Soc. Rev.* **2009**, *38*, 1450.
(18) Li, S.-L.; Xu, Q. *Energy Environ. Sci.* **2013**, *6*, 1656.
(19) Miner, E. M.; Fukushima, T.; Sheberla, D.; Sun, L.; Surendranath, Y.; Dincă, M. *Nat. Commun.* **2016**, *7*, 10942.
(20) Na, K.; Choi, K. M.; Yaghi, O. M.; Somorjai, G. A. *Nano Lett.* **2014**, *14*, 5979.
(21) Xiao, D. J.; Bloch, E. D.; Mason, J. A.; Queen, W. L.; Hudson, M. R.; Planas, N.; Borycz, J.; Dzubak, A. L.; Verma, P.; Lee, K.; Bonino, F.; Crocellà, V.; Yano, J.; Bordiga, S.; Truhlar, D. G.; Gagliardi, L.; Brown, C. M.; Long, J. R. *Nat. Chem.* **2014**, *6*, 590.
(22) Wu, D.; Guo, Z.; Yin, X.; Pang, Q.; Tu, B.; Zhang, L.; Wang, Y.-G.; Li, Q. *Adv. Mater.* **2014**, *26*, 3258.
(23) Kornienko, N.; Zhao, Y.; Kley, C. S.; Zhu, C.; Kim, D.; Lin, S.; Chang, C. J.; Yaghi, O. M.; Yang, P. *J. Am. Chem. Soc.* **2015**, *137*, 14129.
(24) Hod, I.; Deria, P.; Bury, W.; Mondloch, J. E.; Kung, C.-W.; So, M.; Sampson, M. D.; Peters, A. W.; Kubiak, C. P.; Farha, O. K.; Hupp, J. T. *Nat. Commun.* **2015**, *6*, 8304.
(25) Hu, H.; Guan, B.; Xia, B.; Lou, X. W. *J. Am. Chem. Soc.* **2015**, *137*, 5590.
(26) Hu, H.; Han, L.; Yu, M.; Wang, Z.; Lou, X. W. *Energy Environ. Sci.* **2016**, *9*, 107.
(27) Han, L.; Yu, X. Y.; Lou, X. W. D. *Adv. Mater.* **2016**, *28*, 4601.
(28) Wu, H. B.; Xia, B. Y.; Yu, L.; Yu, X. Y.; Lou, X. W. *Nat. Commun.* **2015**, *6*, 6512.
(29) Wurster, B.; Grumelli, D.; Hötger, D.; Gutzler, R.; Kern, K. *J. Am. Chem. Soc.* **2016**, *138*, 3623.
(30) Zhang, T.; Lin, W. *Chem. Soc. Rev.* **2014**, *43*, 5982.
(31) Wang, S.; Yidong, H.; Sen, L.; Xinchen, W. *Nanoscale* **2014**, *6*, 9930.
(32) Manna, P.; Debgupta, J.; Bose, S.; Das, S. K. *Angew. Chem., Int. Ed.* **2016**, *55*, 2425.
(33) Liao, P. Q.; Chen, H.; Zhou, D. D.; Liu, S. Y.; He, C. T.; Rui, Z.; Ji, H.; Zhang, J. P.; Chen, X. M. *Energy Environ. Sci.* **2015**, *8*, 1011.
(34) Colombo, V.; Galli, S.; Choi, H. J.; Han, G. D.; Maspero, A.; Palmisano, G.; Masciocchi, N.; Long, J. R. *Chem. Sci.* **2011**, *2*, 1311.
(35) Park, K. S.; Ni, Z.; Cote, A. P.; Choi, J. Y.; Huang, R.; Uribe-Romo, F. J.; Chae, H. K.; O'Keeffe, M.; Yaghi, O. M. *Proc. Natl. Acad. Sci. U. S. A.* **2006**, *103*, 10186.
(36) Qin, J.-S.; Du, D.-Y.; Guan, W.; Bo, X.-J.; Li, Y.-F.; Guo, L.-P.; Su, Z.-M.; Wang, Y.-Y.; Lan, Y.-Q.; Zhou, H.-C. *J. Am. Chem. Soc.* **2015**, *137*, 7169.
(37) Iliev, M. N.; Hadjiev, V. G.; Iniguez, J.; Pascual, J. *Acta Phys. Pol., A* **2009**, *116*, 19.
(38) Tang, C.-W.; Wang, C.-B.; Chien, S.-H. *Thermochim. Acta* **2008**, *473*, 68.
(39) Feng, J. X.; Ding, L. X.; Ye, S. H.; He, X. J.; Xu, H.; Tong, Y. X.; Li, G. R. *Adv. Mater.* **2015**, *27*, 7051.
(40) Morris, W.; Leung, B.; Furukawa, H.; Yaghi, O. K.; He, N.; Hayashi, H.; Houndonougbo, Y.; Asta, M.; Laird, B. B.; Yaghi, O. M. *J. Am. Chem. Soc.* **2010**, *132*, 11006.
(41) Tian, J.-Q.; Liu, Q.; Asiri, A. M.; Sun, X.-P. *J. Am. Chem. Soc.* **2014**, *136*, 7587.
(42) Sun, L.; Hendon, C. H.; Minier, M. A.; Walsh, A.; Dinca, M. *J. Am. Chem. Soc.* **2015**, *137*, 6164.
(43) Zhang, Y.; Liao, W.-Q.; Ye, H.-Y.; Fu, D.-W.; Xiong, R.-G. *Cryst. Growth Des.* **2013**, *13*, 4025.
(44) Kim, S. W.; Kwon, B. J.; Park, J. H.; Hur, M. G.; Yang, S. D.; Jung, H. *Bull. Korean Chem. Soc.* **2010**, *31*, 910.
(45) Ullman, A. M.; Brodsky, C. N.; Li, N.; Zheng, S.-L.; Nocera, D. G. *J. Am. Chem. Soc.* **2016**, *138*, 4229.
(46) Zhang, B.; Zheng, X.; Voznyy, O.; Comin, R.; Bajdich, M.; Garcia-Melchor, M.; Han, L.; Xu, J.; Liu, M.; Zheng, L.; Garcia de Arquer, F. P.; Dinh, C. T.; Fan, F.; Yuan, M.; Yassitepe, E.; Chen, N.; Regier, T.; Liu, P.; Li, Y.; De Luna, P.; Janmohamed, A.; Xin, H. L.; Yang, H.; Vojvodic, A.; Sargent, E. H. *Science* **2016**, *352*, 333.
(47) Ahn, H. S.; Tilley, T. D. *Adv. Funct. Mater.* **2013**, *23*, 227.
(48) Kanan, M. W.; Nocera, D. G. *Science* **2008**, *321*, 1072.
(49) Wang, J.; Cui, W.; Liu, Q.; Xing, Z.; Asiri, A. M.; Sun, X. *Adv. Mater.* **2016**, *28*, 215.
(50) Zhang, G. Q.; Wu, H. B.; Hoster, H. E.; Chan-Park, M. B.; Lou, X. W. D. *Energy Environ. Sci.* **2012**, *5*, 9453.
(51) Jin, H.; Wang, J.; Su, D.; Wei, Z.; Pang, Z.; Wang, Y. *J. Am. Chem. Soc.* **2015**, *137*, 2688.
(52) Zhu, Y.-P.; Liu, Y.-P.; Ren, T.-Z.; Yuan, Z.-Y. *Adv. Funct. Mater.* **2015**, *25*, 7337.

DOI: 10.1021/jacs.6b03125
J. Am. Chem. Soc. 2016, 138, 8336−8339